Cauchy Functions Compared to the Gaussian for X-Ray Powder Diffraction Line Profile Fitting: An Exercise

Hans Hermann Otto

Materialwissenschaftliche Kristallographie, Clausthal University of Technology, Clausthal-Zellerfeld, Lower Saxony, Germany

E-mail: hhermann.otto@web.de

Abstract

The best-known profile function is the *Gaussian* function, which can be used, for instance, to fit successfully optical absorption bands or neutron scattering patterns. However, peaks of *X*-ray powder pattern can hardly be fitted well with such a simple function. Whereas combined functions are widely in use for such purpose, we applied *Cauchy* functions to fit our well resolved *Guinier* powder diffraction data. The *Cauchy* function of second order is well suited and will be described in more detail as a didactic exercise in crystallography as well as mathematics. In addition, a profile function with an exotic non-integer exponent based on the golden mean is supplemented. This contribution will be continuously revised before its final publication to react of *Fewster*'s new diffraction theory that will change the matter in future. As an example beyond crystallography the author fitted German Covid-19 data to correlate virus infection peak maxima with causal events.

Keywords: Line Profile Functions, Gaussian Function, Cauchy Functions, Full Width at Half Maximum, X-Ray Diffraction, UV-VIS.

1. Introduction

Profile functions of different full width at half maximum were used as so called line functions to decompose optical spectra or *X*-ray powder diffraction patterns. Normalized to unity, they will be simply multiplied with the line intensity to represent the full information. Fit parameters are the location of the line, its intensity, and the width, respectively. In this exercise, we don't consider combined functions as used today in *Rietfelt* refinement, but the series of *Cauchy* functions of ever steeper profile, where the first number of the series (order one) is alternatively known as *Lorentzian* profile function. *Mitra* [1] recently described theoretical models of diffraction line profiles in detail. However, we used the second order *Cauchy* function successfully to decompose the highly resolved *X*-ray powder diffraction

patterns, taken with our double-radius *Guinier* diffractometer with imaging plate (IP) detector [2] [3].

Baron *Augustin-Louis Cauchy* was a French mathematician and physicist (* Aug. 23. 1789 in Paris, † May 23. 1857 in Sceaux, France). In this contribution, we deal with two findings of this great researcher, the *Cauchy* profile functions beside the *Cauchy* integral formula to verify their half-peak widths. In addition, we contribute a sort of Cauchy line functions with non-integer order.

2. Cauchy Functions

Cauchy line profile functions P_n of order n are represented by the following equation:

$$P_n = \frac{B}{a} \cdot \{1 + (\frac{t-t_o}{a})^2\}^{-n},$$ (1)

where w is the effective half-width and a the fictive one, with $a = \frac{w}{c} = \frac{w_F}{2c}$, $w_F = 2w$ represents the full width at half maximum (*FWHM*).

Peak (line) maximum is given for $t = t_o$

$$P_{n,max} = \frac{B}{a}$$ (2)

It yields further for $n = 1$: $\qquad B = 1/\pi , \quad c = 1$ (3)

$\qquad\qquad n = 2$: $\qquad B = 2/\pi, \quad c = \sqrt{\sqrt{2} - 1} = 0.64359425\ldots$ (4)

The constant c can be verified, if we set $w = t_{1/2} - t_o$ for $P_{max}/2$.

Doing this, we can find the constant c for the third order *Cauchy* function, because $c = \frac{t_{1/2} - t_o}{a}$.

$$\frac{P_3(max)}{2} = \frac{B}{2a} = \frac{B}{a} \frac{1}{[1+(\frac{t_{1/2}-t_o}{a})^2]^3} = \frac{B}{a} \frac{1}{[1+c^2]^3}$$ (5)

Solving for c gives $\qquad\qquad c = \sqrt{\sqrt[3]{2} - 1} = 0.509825$

For the *Cauchy* functions $P_1(t)$ respectively $P_2(t)$ we get

$$P_1(t) = \frac{w}{\pi(w^2 + (t-t_o)^2)}$$ (6)

$$P_2(t) = \frac{2c}{\pi \cdot w \left[1 + c^2(\frac{t-t_o}{w})^2\right]^2}$$ (7)

Integration of the *Cauchy* function of first order yields with the substitution $x = t - t_o$

$$\int_{-\infty}^{\infty} \frac{w}{\pi} (w^2 + x^2)^{-1} dx = \frac{w}{\pi} \cdot \int_{-\infty}^{\infty} \frac{1}{w^2+x^2} dx = \frac{w}{\pi} \cdot \left[\frac{2}{w} \text{atan}\left(\frac{x}{w}\right)\right]_o^{\infty} = \frac{2}{\pi} \left[\frac{\pi}{2} - 0\right] = 1$$ (8)

2

Therefore, this integral is normalized to unity.

Integration of the *Cauchy* function of second order yields

$$\int_{-\infty}^{\infty} \frac{B}{a} \frac{1}{(1+[(\frac{t-t_0}{a})^2]^2} \, dt = B \cdot \int_{-\infty}^{\infty} \frac{dx}{(1+x^2)^2} \tag{9}$$

when simplifying with the substitution $x = (t - t_o)/a$ and $dx = dt/a$ or $dt = a \cdot dx$

The solution gives

$$\int_{-\infty}^{\infty} \frac{dx}{(1+x^2)^2} = [\frac{x}{2(1+x^2)} + \frac{1}{2} \cdot \mathrm{atan}(x)]_{-\infty}^{+\infty} = \frac{\pi}{2} \tag{10}$$

Thus the integral $\int_{-\infty}^{\infty} P_2 \, dt = B \cdot \int_{-\infty}^{\infty} \frac{dx}{(1+x^2)^2} = B \cdot \frac{\pi}{2} = \frac{2}{\pi} \cdot \frac{\pi}{2} = 1$ is also normalized to unity.

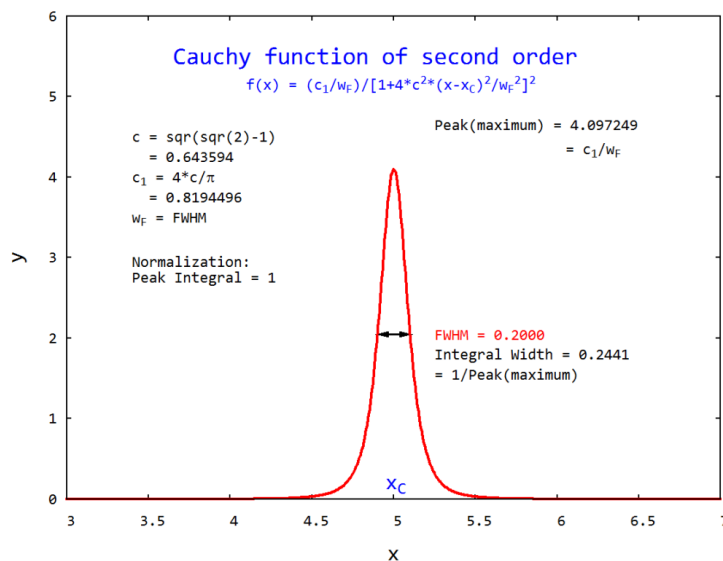The integral width w_i results from the relation

$$P_{max} \cdot w_i = 1 \text{ giving } w_i = 1/P_{max} \tag{11}$$

We get for $n = 1$
$$w_i = \frac{\pi}{2} \cdot w_F = 1.570796 \cdot FWHMP \tag{12}$$
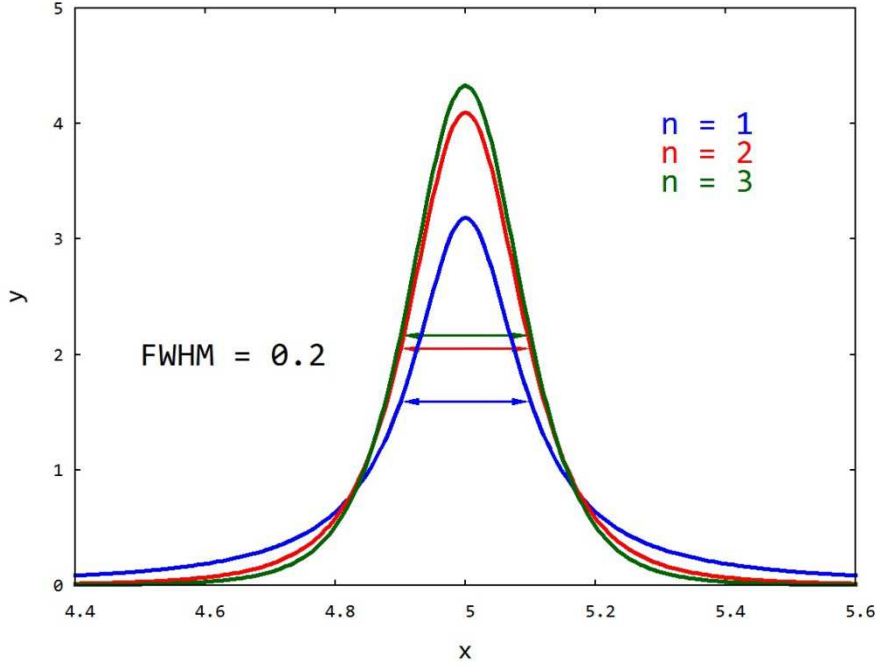
$n = 2$
$$w_i = \frac{\pi}{4c} \cdot w_F = 1.220331 \cdot FWHMP \tag{13}$$

$n = 3$
$$w_i = \frac{3\pi}{16c} \cdot w_F = 1.155394 \cdot FWHMP \tag{14}$$

Cauchy functions were illustrated in the Figures 1 and Figure 2 below.

Figure 1. *Cauchy* function of second order with a chosen *FWHM* = 0.2 and normalized to unity peak integral. The function is symmetric around the center at chosen $x_c = 5$.

3

Figure 2. *Cauchy* functions of order *n* = 1 to 3 with the same *FWHM* = 0.2

3. *Gaussian* Profile Function in Comparison with the *Cauchy* Function of Second Order

This profile function with the smallest width in the base compared to *Cauchy* functions was treated for the sake of completeness. This normal distribution represents the most important continuous probability distribution and has been frequently described in the literature. It is defined as follows

$$f(x) = \frac{1}{\sigma\sqrt{2\pi}}\exp{-\frac{1}{2}\left(\frac{t-t_o}{\sigma}\right)^2} \tag{15}$$

First, we will show that the below given integral is normalized to unity

$$I \coloneqq \frac{1}{\sqrt{2\pi}}\int_{-\infty}^{\infty}\exp\left(-\frac{1}{2}t^2\right)dt \tag{16}$$

According to *Evesons* [4] one may write in a higher dimension

$$I^2 = \frac{1}{2\pi}\int_{-\infty}^{\infty}\exp\left(-\frac{1}{2}x^2\right)dx\int_{-\infty}^{\infty}\exp\left(-\frac{1}{2}y^2\right)dy = \frac{1}{2\pi}\int_{-\infty}^{\infty}\exp{-\frac{1}{2}(x^2+y^2)}\,dxdy \tag{17}$$

Using now polar coordinates one yields

$$I^2 = \frac{1}{2\pi}\int_{0}^{\infty}\int_{0}^{2\pi}\exp\left(-\frac{1}{2}r^2\right)r\,d\varphi dr = \int_{0}^{\infty}\exp\left(-\frac{1}{2}r^2\right)r\,dr = -\left[\exp\left(-\frac{1}{2}r^2\right)\right]_{r=0}^{\infty} = 1 \tag{18}$$

Thus, the integral is

$$I = \sqrt{I^2} = 1 \tag{19}$$

4

For purposes of programming applying the least squares refinement routine, we reformulate the equation to get the full width at half maximum w_F, thereby the area under the integral must remain unity. We get the following equation

$$f(x) = \frac{c_1}{w_F} \cdot \exp\left(-\frac{c_2(x-x_c)^2}{w_F^2}\right),$$
(20)

where the constants are $\quad c_1 = \dfrac{2\sqrt{(2\ln(2))}}{\sqrt{(2\pi)}} = \dfrac{w_F}{w_i} = 0.93943728 \quad$ and $\quad c_2 = 4 \cdot \ln(2)$

Figure 3 compares the normalized *Gaussian* function with the *Cauchy* function of second order, both with the same peak height but different *FWHM*. The *Cauchy* function shows reduced *FWHM* compared to the *Gaussian*, but smeared broader out in the base to give the same unit integral area (see also Figure 4). Therefore, be cautious with a statement like 'the *Gaussian* has smaller half-width than *Cauch*y functions', because this is only true near the base of the function.

We use both functions alternatively in our *Profile-C2G.bas* program (pre-published in *Researchgate.net*), replacing the scattering angle 2θ for *x*, and the measured *X-ray* intensity for *y*, respectively [5]. If you want to use the program to fit *UV-VIS* data, then you have to choose the *Gaussian* option.
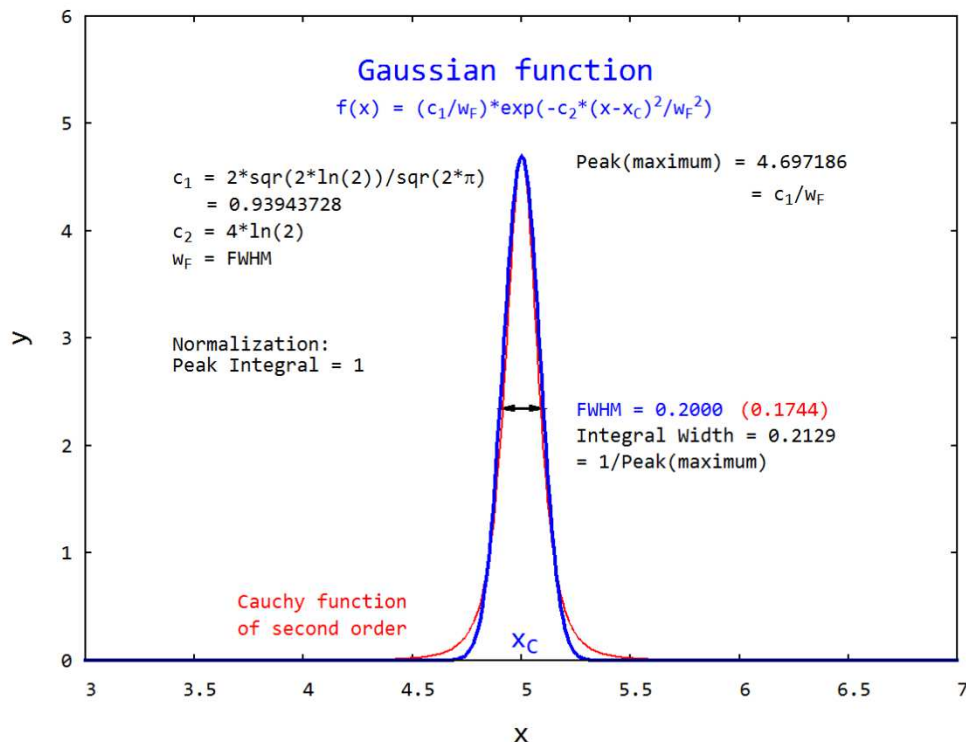
Figure 3. Normalized *Gaussian* profile function (blue) in comparison with a *Cauchy* function of second order (red) with the same peak height, showing then different *FWHM*.
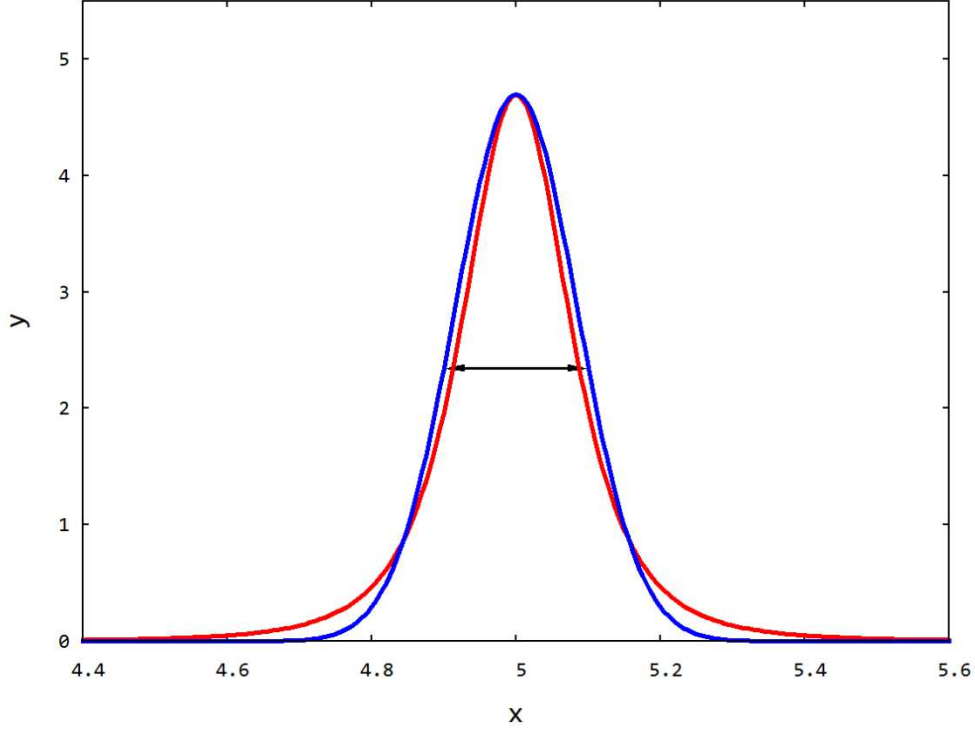
Figure 4. Enlarged image detail from Figure 2
Gaussian blue, *Cauchy* function of second order red, the arrow shows the position at *FWHM*.

4. Convolution of *Gaussian* respectively *Cauchy* Functions

Results of such calculation can be useful when the apparatus contribution to the broadening of an *X*-ray reflection is to be calculated out, for example to determine the true crystallite size. Two peaks represented by the same function type can be convoluted and deliver on the back transformation of the *Fourier* transform the following result for the width at half maximum considering the combined peak.

Cauchy function of order 1: $\qquad w = w_1 + w_2$ (21)

Cauchy function of order 2 [6]: $\qquad w^{\sqrt{2}} = w_1^{\sqrt{2}} + w_2^{\sqrt{2}}$ (22)

Gaussian function [7]: $\qquad w^2 = w_1^2 + w_2^2$ (23)

The convolution of the functions $f(t)$ and $g(t)$ reads as

$$f(t) * g(t) = \int_{-\infty}^{\infty} f(\tau)g(t - \tau)d\tau \qquad (24)$$

The *Fourier* transform of the convolution product represents the product of the *Fourier* transforms of both starting functions

$$\mathcal{F} = \int_{-\infty}^{\infty} e^{-i\omega t}\left[\int_{-\infty}^{\infty} f(\tau)g(t - \tau)d\tau\right] dt = F(\omega)G(\omega) \qquad (25)$$

6

where in the case of the *Gaussian* $F(\omega) = \exp(-\frac{\omega^2\sigma_1^2}{2})$ respectively $G(\omega) = \exp\left(-\frac{\omega^2\sigma_2^2}{2}\right)$,

$$F(\omega)G(\omega) = \exp\left(-\frac{\omega^2(\sigma_1^2+\sigma_2^2)}{2}\right). \tag{26}$$

In this way the convolution resulted in

$$f(x) * g(x) = \frac{1}{\sqrt{\sigma_1{}^2+\sigma_2{}^2}\sqrt{2\pi}}\exp[-\frac{1}{2}(\frac{t-t_o}{\sigma_1^2+\sigma_2^2})^2], \tag{27}$$

leading for $w = \sigma$ to the final result

$$w^2 = w_1^2 + w_2^2 \tag{see 23}$$

For the first order *Cauchy* function we write now $L(t)$ (*Lorentzian*) and substitute $x = t - t_o$

$$L(x) = \frac{w}{\pi(w^2+x^2)} \tag{28}$$

then apply the *Fourier* transform

$$\mathcal{F}\{L(x)\} = \int_{-\infty}^{\infty}\frac{w}{\pi(w^2+(x)^2)}\,e^{-ikx}dx = \frac{w}{\pi}\int_{-\infty}^{\infty}\frac{e^{-ikx}}{(x+iw)(x-iw)}dx \tag{29}$$

From *Cauchy*'s integral formula it follows [8]:

Case $k < 0$: the contour integral is taken counter-clockwise

$$\mathcal{F}\{L(x)\} = \frac{w}{\pi}\oint\frac{e^{-ikz}}{z+iw}\cdot\frac{1}{z-iw}dz = \frac{2\pi iw}{\pi}\frac{e^{-ik(iw)}}{2iw} = e^{wk} \tag{30}$$

Case $k > 0$: the contour integral is taken clockwise (add minus to the integral!)

$$\mathcal{F}\{L(x)\} = \frac{w}{\pi}\oint\frac{e^{ikz}}{z-iw}\cdot\frac{1}{z+iw}dz = -\frac{2\pi iw}{\pi}\frac{e^{ik(-iw)}}{-2iw} = e^{-wk}, \tag{31}$$

Finally we get $\quad\quad\quad\quad \mathcal{F}\{L(x)\} = e^{-w|k|} \tag{32}$

Then we obtain for the product of two functions

$$\mathcal{F}\{L_1(x)\}\mathcal{F}\{L_2(x)\} = e^{-ik(w_1+w_2)}. \tag{33}$$

Because this product represents the convolution of two *Lorentzian* type functions, the convoluted function has a half-width of

$$w = w_1 + w_2$$

This result confirms Equation 21.

The proof for the half-width of convoluted *Cauchy* functions of order two according to Equation 22 by a sophisticated decomposition of the integrand will be supplemented soon. Many years ago, we had analytically verified the validity of this relation [6].

5. *Cauchy*-Type Line Profile Function with Exotic Non-Integer Order

Tentatively, we can try to work also with a non-integer order for the *Cauchy* line profile function, for instance choosing an order between 2 and 3. A proposal is

$\varphi^{-2} = 2.6180339887 \ldots$, where $\varphi = \frac{\sqrt{5}-1}{2} = 0.6180339887 \ldots$ is the golden mean.

The quality to be exotic will only be used in context with *Cauchy* functions, not generally quoting the importance of this most irrational number in biology, cosmology, music, art, finance, and medicine.

This function is represented by

$$P_\varphi = \frac{B \cdot c}{w} \cdot \{1 + c^2 \cdot (\frac{t-t_o}{w})^2\}^{-n}, n = \varphi^{-2}, \tag{34}$$

$$\text{where } B \approx \frac{3}{2\pi\varphi} = 0.772554 \ldots, \quad c = \sqrt{2^{\varphi \cdot \varphi} - 1} = 0.5505601 \ldots \tag{35}$$

However, the integral of P_φ is somewhat smaller than 1

$$\int_{-\infty}^{\infty} P_\varphi \, dt = 0.998 \ldots \approx 1 \tag{36}$$

One can apply instead of $B = \frac{3}{2\pi\varphi}$ an expanded form for B to approximate the integral more exactly to unity

$$B \approx \frac{1}{2\pi} [3\varphi^{-1} + (\frac{\varphi}{3+\pi})^2 + \frac{1}{5}(\frac{\varphi}{3+\pi})^4]. \tag{37}$$

With this expansion that represents not the exact solution, the integral intensity deviates only marginally from 1

$$\int_{-\infty}^{\infty} P_\varphi \, dt = 0.99965 \ldots \tag{38}$$

Such profile function near the *Gaussian* may find application in special cases concerning statistics, deciphering secrets of our cosmos or approaches in financial research.

5. Conclusions

The fundamental line profile functions for *X*-ray powder diffraction or neutron powder scattering have been summarized as an exercise, and small odds in previously published contributions misleading the reader have been tried to avoid. We extended the *Cauchy* line profile series with a function of non-integer order based on the golden mean. This contribution is continuously being revised also in light of *Fewster*'s new diffraction theory [9], before a final publication will be envisaged. As an example beyond crystallography Germany's active Covid-19 infection cases were fitted with *Cauchy* respectively *Gaussian* functions [10].

References

[1] Mitra, G. B. (2014) Theoretical Model of Diffraction Line Profiles as Combination of Gaussian and Cauchy Distributions. *Journal of Crystallization Process and Technology* **4**, 145-155.

[2] Otto, H. H. and W. Hofmann, W. (1996) Construction of a double radius Guinier diffractometer using Mo-K$_{\alpha1}$ radiation and a one- or two-dimensional detection system. *Journal of Applied Crystallography* **29**, 495-497.

[3] Otto, H. H. (2018) X-Ray Powder Diffraction: Why Not Use CuKß Radiation? *Journal of Analytical Sciences, Methods and Instrumentation* **8**, 37-47.

[4] Lee, P. M. (2011) The probability integral. *University of York*, *Department of Mathematics*. The author cited a private communication of S. P. Evesons (2005).

[5] Otto, H. H. (2018) The Basic Program Profile-C2G.bas for X-Ray Powder Diffraction Line Profile Analysis. *Researchgate.net*, Pre-Publication.

[6] Otto, H. H. (1992) Lecture about X-Ray Diffraction Methods. TU Clausthal, Germany

[7] Bromiley, P. A. (2003) Products and Convolutions of Gaussian Probability Density Functions. *Tina Memo* No 2003-003, last updated 11/9/2013. See also references therein.

[8] Hosemann, R. and Bagchi, S. N. (1962) Direct Analysis of Diffraction by Matter. *North-Holland Publishing Company*, Amsterdam, pp.186 ff.

[9] Fewster, P. F. (2013) A new theory for X-ray diffraction. *Acta Crystallographica* **A70**, 257-282.

[10] Otto, H. H. (2019) Development of Germany's Active Covid-19 Infection Cases. *Researchgate*, 1-11.